

# A Study of Generation of Classical Squeezed States Using Stochastic Force, and Their Applications in Building Highly Efficient Heat Engines

**Archisman Panigrahi** (archismanp@iisc.ac.in)

Dept. of Undergraduate Programme, Indian Institute of Science, Bangalore, India

SR No. - 11-01-00-10-91-17-1-14503

KVPY SA Fellow, 2015, KVPY Registration No. - SA-1510017

Under the Guidance of

**Prof. H. R. Krishnamurthy**

Dept. of Physics, Indian Institute of Science, Bangalore, India

2019

## Abstract

It is a challenging task to make efficient heat engines. The Carnot limit [1] provides an upper bound for the efficiency of a heat engine. It was claimed in a recent paper [2] that it is possible to experimentally surpass the Carnot limit using non-equilibrium reservoirs, and the second law of thermodynamics was not violated due to the non-equilibrium nature of the reservoirs. There was a claim that a certain kind of stochastic forcing gave rise to classical squeezed states, which can be utilized to make such a heat engine. In this report, that claim is critically analyzed, and the sense in which the Carnot efficiency is surpassed, and why the second law is still not violated is explained.



## Certificate

This is to certify that Archisman Panigrahi (SR No. 11-01-00-10-91-17-1-14503), undergraduate student at Indian Institute of Science, did his 2019 summer research project titled *A Study of Generation of Classical Squeezed States Using Stochastic Force, and Their Applications in Building Highly Efficient Heat Engines* under my guidance.

**Prof. H. R. Krishnamurthy**

Department of Physics

Indian Institute of Science, Bangalore.

## Acknowledgment

I am grateful to Prof. H. R. Krishnamurthy for guiding me in this project and for providing his valuable time to explain many topics to me. I am also grateful to him for growing my interest in different branches of Condensed Matter Physics.

I am thankful to D.S.T. and K.V.P.Y. for providing me scholarship.

## Contents

<b>1</b>	<b>Introduction</b>	<b>5</b>
<b>2</b>	<b>Theory of the for Brownian Harmonic oscillator</b>	<b>6</b>
2.1	Coherent states of a quantum harmonic oscillator . . . . .	6
2.2	Squeezed states of a quantum harmonic oscillator . . . . .	8
2.2.1	Expansion of squeezed state in eigenstate basis and its time evolution	10
2.3	Classical Brownian motion under harmonic potential . . . . .	14
2.3.1	Langevin equation . . . . .	14
2.3.2	Explanation of the nature of correlation of the stochastic force . . .	14
2.3.3	Fluctuation dissipation theorem and the claim . . . . .	15
<b>3</b>	<b>Proof of the claim</b>	<b>16</b>
3.0.1	Preliminaries . . . . .	17
3.0.2	Calculation of Fourier transformed position and momentum . . . .	18
3.1	Calculation of variance in position . . . . .	19
3.2	Calculation of covariance in position and momentum . . . . .	19
3.3	Calculation of variance in momentum . . . . .	20
3.4	Rotating coordinates . . . . .	21

<b>4</b>	<b>Other methods to get this result</b>	<b>23</b>
4.1	Directly integrating the equations in Mathematica . . . . .	23
4.2	Verification using a simulation . . . . .	23
<b>5</b>	<b>How the Heat Engine works</b>	<b>23</b>
5.1	How the force is applied . . . . .	23
5.2	How the quantities are measured . . . . .	24
5.3	How it is used as a heat engine . . . . .	25
5.4	How efficiency is measured . . . . .	25
<b>6</b>	<b>Explanation of different effective temperatures and the reason for surpassing the second law</b>	<b>26</b>
<b>7</b>	<b>Conclusion</b>	<b>27</b>

# 1 Introduction

The classical limit for the maximum achievable efficiency of an ideal heat engine running between temperatures  $T_{hot}$  and  $T_{cold}$  is given by Carnot’s formula  $\eta_{Carnot} = 1 - \frac{T_{cold}}{T_{hot}}$ . Being reversible, the Carnot engine which achieves this efficiency is infinitely slow, and there are frictional dissipations in the real world. As a result, the efficiency of real, irreversible engines is a small fraction of this ideal formula. Nano engines based on the principles of Quantum Mechanics can achieve much higher efficiencies than their classical counterparts [3] and can have efficiency close to the Carnot limit. These engines can be realized in many forms including ion traps [4], bacterial reservoirs [5], harmonic oscillators [6]. It has been shown both theoretically [7] and experimentally [2] that the efficiencies of engines realized using “squeezed harmonic oscillators” can even surpass the Carnot limit, without violating the second law of thermodynamics. In this report, it will be elaborated in which sense the Carnot limit is surpassed, and why the second law is not violated. To see how the experiment [2] was done, let us recap squeezed states of harmonic oscillator

and Brownian motion.

## 2 Theory of the for Brownian Harmonic oscillator

Before we discuss squeezed states, let us review “Coherent states” of a harmonic oscillator.

### 2.1 Coherent states of a quantum harmonic oscillator

The position and momentum of classical harmonic oscillator (a particle of mass  $m$  in potential  $\frac{1}{2}m\omega^2x^2$ , basically a spring-mass system) oscillate with period  $\omega$ , its natural frequency. However, in quantum mechanics, the expectation value of position or momentum in an eigenstate of the Hamiltonian does not change with time.

For the harmonic oscillator, the Hamiltonian is  $\hat{H} = \frac{\hat{p}^2}{2m} + \frac{1}{2}m\omega^2\hat{x}^2$ .

Let the eigenstates of  $\hat{H}$  be denoted by  $|n\rangle$ . It can be shown [8] that it has energy  $E_n = (n + \frac{1}{2})\hbar\omega$ . The state evolves with time as  $|n, t\rangle = e^{-i(n+\frac{1}{2})\omega t} |n, t=0\rangle$ , and the position and momentum coordinate will share equal energies  $(n + \frac{1}{2})\frac{\hbar\omega}{2}$ . And, the expectation values of position and momentum are zero and do not change over time. There exist quantum states in which the expectation values of position and momentum oscillate sinusoidally with time, and the wave packet does not spread with time. These are known as “Coherent states” [9].

Let us define  $x_0 = \sqrt{\frac{\hbar}{m\omega}}$  and  $p_0 = \sqrt{\hbar m\omega}$ , and dimensionless operators  $\hat{X} = \frac{\hat{x}}{x_0}, \hat{P} = \frac{\hat{p}}{p_0}$ . Then we can rewrite

$$\hat{H} = \frac{\hbar\omega}{2}(\hat{X}^2 + \hat{P}^2) \quad (1)$$

Let us define two non Hermitian operators  $\hat{a} = \frac{\hat{X} + i\hat{P}}{\sqrt{2}}$ , and  $\hat{a}^\dagger = \frac{\hat{X} - i\hat{P}}{\sqrt{2}}$ . Then,  $[\hat{a}, \hat{a}^\dagger] = 1$ , and the Hamiltonian can be written as  $\hat{H} = \hbar\omega(\hat{a}^\dagger\hat{a} + \frac{1}{2})$ .  $\hat{a}^\dagger$  and  $\hat{a}$  are known as “creation” and “annihilation” operators, respectively, because they act on the eigenstates as follows.

$$\hat{a}|n\rangle = \sqrt{n}|n-1\rangle \quad (2)$$

$$\hat{a}^\dagger|n\rangle = \sqrt{n+1}|n+1\rangle \quad (3)$$

We can define  $\hat{N} = \hat{a}^\dagger \hat{a}$ , and then,  $\hat{N}|n\rangle = n|n\rangle$ , denoting the number of excitations (e.g. photons or phonons) in the system. The creation and annihilation operators can be viewed as operators which create or destroy such an excitation, respectively, hence their name.

The operator  $\hat{a}$  acts on  $|0\rangle$  (the vacuum state) to give the zero vector of the Hilbert space. However, there exist states which are eigenstates of the annihilation operator, and these are the coherent states.

Let

$$\hat{a}|\alpha\rangle = \alpha|\alpha\rangle \quad (4)$$

where  $\alpha$  is a complex number, and  $|\alpha\rangle$  is a coherent state. Since  $|n\rangle$  form a basis of the Hilbert space,  $\exists c_n \in \mathbb{C}$ , such that

$$|\alpha\rangle = \sum_{n=0}^{\infty} c_n |n\rangle \quad (5)$$

$$\begin{aligned} \text{From equations (4) and (5), we get, } & \sum_{n=0}^{\infty} c_n \hat{a} |n\rangle = \sum_{n=0}^{\infty} \alpha c_n |n\rangle \\ \implies & \sum_{n=1}^{\infty} c_n \sqrt{n} |n-1\rangle = \sum_{n=0}^{\infty} \alpha c_n |n\rangle \\ \implies & \sum_{n=0}^{\infty} c_{n+1} \sqrt{n+1} |n\rangle = \sum_{n=0}^{\infty} \alpha c_n |n\rangle \\ \implies & c_{n+1} \sqrt{n+1} = \alpha c_n \\ \implies & \frac{c_{n+1} \sqrt{(n+1)!}}{\alpha^{n+1}} = \frac{c_n \sqrt{n!}}{\alpha^n} \\ & = \frac{c_0 \sqrt{0!}}{\alpha^0} \\ \implies & c_n = c_0 \frac{\alpha^n}{\sqrt{n!}} \end{aligned}$$

Since  $\sum_{n=0}^{\infty} |c_n|^2 = 1 \implies c_0 = e^{-\frac{|\alpha|^2}{2}}$ . Finally we get  $|\alpha\rangle = e^{-\frac{|\alpha|^2}{2}} \sum_{n=0}^{\infty} \frac{\alpha^n}{\sqrt{n!}} |n\rangle$ , and  $|\alpha, t\rangle = e^{-\frac{|\alpha|^2 + i\omega t}{2}} \sum_{n=0}^{\infty} \frac{(\alpha e^{-i\omega t})^n}{\sqrt{n!}} |n\rangle$ . So the state remains a coherent state over time, only

the parameter  $\alpha$  evolves as  $\alpha(t) = \alpha(0)e^{-i\omega t}$ . Now, in the coherent state  $|\alpha\rangle$ ,

$$\left\{ \begin{array}{l} \langle \hat{a} \rangle = \alpha \\ \langle \hat{a}^\dagger \rangle = \alpha^* \\ \langle x \rangle = x_0 \left\langle \frac{\hat{a} + \hat{a}^\dagger}{\sqrt{2}} \right\rangle = x_0 \frac{\alpha + \alpha^*}{\sqrt{2}} \\ \langle p \rangle = p_0 \left\langle \frac{\hat{a} - \hat{a}^\dagger}{\sqrt{2}i} \right\rangle = p_0 \frac{\alpha - \alpha^*}{\sqrt{2}i} \\ \langle \hat{x}^2 \rangle = x_0^2 \left\langle \frac{\hat{a}^2 + \hat{a}^{\dagger 2} + \hat{a}\hat{a}^\dagger + \hat{a}^\dagger\hat{a}}{2} \right\rangle = \frac{\alpha^2 + \alpha^{*2} + 2|\alpha|^2 + 1}{2} x_0^2 \\ \langle \hat{p}^2 \rangle = p_0^2 \left\langle \frac{\hat{a}^2 + \hat{a}^{\dagger 2} - \hat{a}\hat{a}^\dagger - \hat{a}^\dagger\hat{a}}{-2} \right\rangle = \frac{2|\alpha|^2 + 1 - \alpha^2 - \alpha^{*2}}{2} p_0^2 \\ \langle E \rangle = \frac{\hbar\omega}{2}(\hat{a}^\dagger\hat{a} + 1) = \frac{\hbar\omega}{2}(|\alpha|^2 + 1) \\ (\Delta x)^2 = \frac{x_0^2}{2} \\ (\Delta p)^2 = \frac{p_0^2}{2} \\ \Delta x \cdot \Delta p = \frac{x_0 p_0}{2} = \frac{\hbar}{2} \end{array} \right. \quad (6)$$

Let  $\alpha = |\alpha|e^{i\phi}$ . Then,  $\langle x \rangle(t) = \sqrt{2}x_0 \text{Re}\{\alpha(t)\} = \sqrt{2}x_0|\alpha| \cos(\phi - \omega t)$ , and  $\langle p \rangle(t) = \sqrt{2}p_0 \text{Im}\{\alpha(t)\} = \sqrt{2}p_0|\alpha| \sin(\phi - \omega t)$ . The total energy, the standard deviations in position and momentum remain constant, while the expectation values of position and momentum vary sinusodially with time, just like for a classical particle. Solving the first order differential equation obtained from (4) in the position basis, it can be easily shown that the wave function  $\psi_\alpha(x) = \langle x|\alpha \rangle$  is a Gaussian of fixed variance  $\frac{x_0^2}{2}$ , centered about a mean  $\langle x \rangle$  which evolves sinusodially with time.

## 2.2 Squeezed states of a quantum harmonic oscillator

The coherent state behaves like a classical particle in a harmonic potential, and it has equal uncertainty in position and momentum. However, there exist states which have different values of standard deviation in position and momentum coordinates. In the next section, we will see that these uncertainties are related to the effective temperature in these coordinates, and this can be utilized to prepare efficient heat engines. Let us define

$$\hat{Q} = \lambda \hat{a} + \mu \hat{a}^\dagger \quad (7)$$



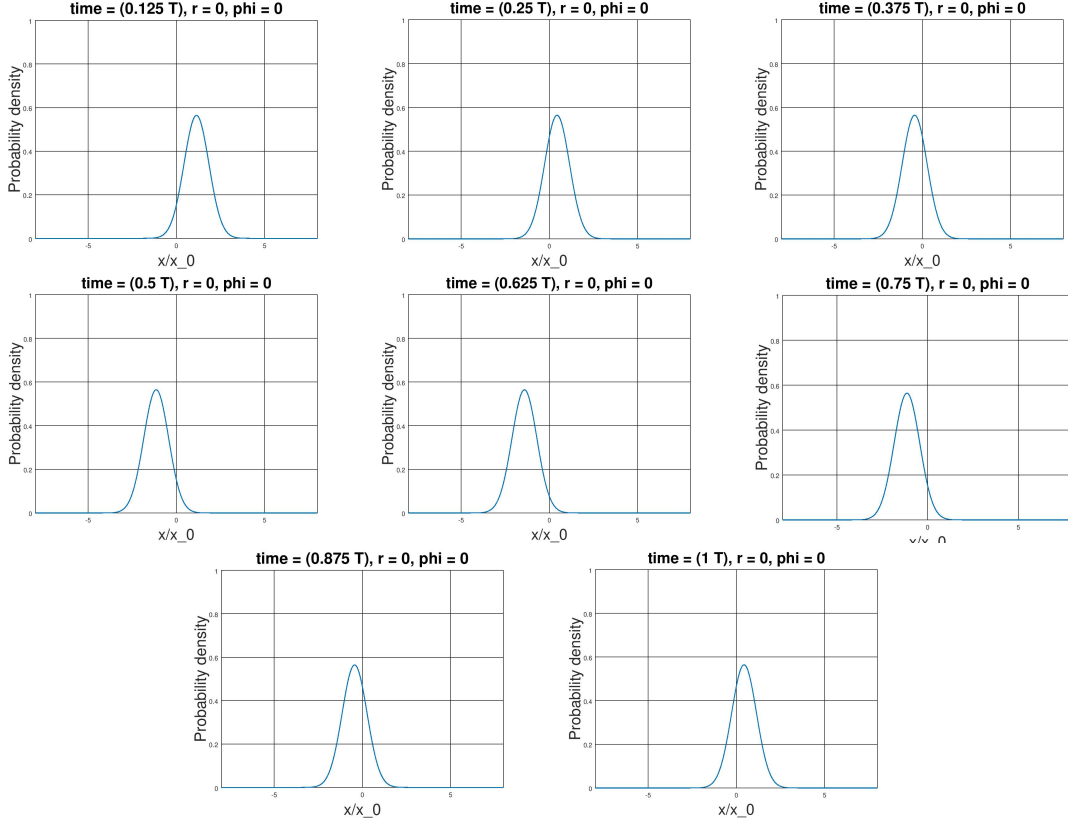


**Figure 1:** Time evolution of probability density of a coherent state.  $T = \frac{2\pi}{\omega}$

where  $|\lambda|^2 - |\mu|^2 = 1$ . Let  $\lambda = \cosh(r)$ ,  $\mu = \sinh(r)e^{i\phi}$ , where  $r, \phi \in \mathbb{R}$ . The eigenstates of  $\hat{Q}$  are defined as the squeezed states [10]. We have,

$$\begin{pmatrix} \hat{Q} \\ \hat{Q}^\dagger \end{pmatrix} = \begin{pmatrix} \lambda & \mu \\ \mu^* & \lambda^* \end{pmatrix} \begin{pmatrix} \hat{a} \\ \hat{a}^\dagger \end{pmatrix}$$

Inverting, we get,

$$\begin{pmatrix} \hat{a} \\ \hat{a}^\dagger \end{pmatrix} = \begin{pmatrix} \lambda^* & -\mu \\ -\mu^* & \lambda \end{pmatrix} \begin{pmatrix} \hat{Q} \\ \hat{Q}^\dagger \end{pmatrix} \quad (8)$$

Therefore,  $\frac{\hat{x}}{x_0} = \frac{\lambda^* - \mu^*}{\sqrt{2}}\hat{Q} + \frac{\lambda - \mu}{\sqrt{2}}\hat{Q}^\dagger$  and  $\frac{\hat{p}}{p_0} = \frac{\lambda^* + \mu^*}{\sqrt{2}i}\hat{Q} - \frac{\lambda + \mu}{\sqrt{2}i}\hat{Q}^\dagger$ .

$$[\hat{Q}, \hat{Q}^\dagger] = [\lambda\hat{a} + \mu\hat{a}^\dagger, \lambda^*\hat{a}^\dagger + \mu^*\hat{a}] = |\lambda|^2 - |\mu|^2 = 1.$$

$$\left(\frac{\hat{x}}{x_0}\right)^2 = \left(\frac{\lambda^* - \mu^*}{\sqrt{2}}\right)^2 \hat{Q}^2 + \left(\frac{\lambda - \mu}{\sqrt{2}}\right)^2 \hat{Q}^{\dagger 2} + \frac{|\lambda - \mu|^2}{2}(2\hat{Q}^\dagger\hat{Q} + 1)$$

$$\left(\frac{\hat{p}}{p_0}\right)^2 = \frac{|\lambda + \mu|^2}{2}(2\hat{Q}^\dagger\hat{Q} + 1) - \left(\frac{\lambda^* + \mu^*}{\sqrt{2}}\right)^2 \hat{Q}^2 - \left(\frac{\lambda + \mu}{\sqrt{2}}\right)^2 \hat{Q}^{\dagger 2}$$

Let  $\hat{Q}|s\rangle = s|s\rangle$  be a squeezed state. For this state, we get the following results.

$$\left\langle \frac{\hat{x}}{x_0} \right\rangle = \frac{\lambda^* - \mu^*}{\sqrt{2}}s + \frac{\lambda - \mu}{\sqrt{2}}s^*$$

$$\begin{aligned}
\left\langle \frac{\hat{p}}{p_0} \right\rangle &= \frac{\lambda^* + \mu^*}{\sqrt{2}i} s - \frac{\lambda + \mu}{\sqrt{2}i} s^* \\
\left\langle \frac{\hat{x}^2}{x_0^2} \right\rangle &= \left( \frac{\lambda^* - \mu^*}{\sqrt{2}} \right)^2 s^2 + \left( \frac{\lambda - \mu}{\sqrt{2}} \right)^2 s^{*2} + \frac{|\lambda - \mu|^2}{2} (2|s|^2 + 1) \\
\left\langle \frac{\hat{p}^2}{p_0^2} \right\rangle &= \frac{|\lambda + \mu|^2}{2} (2|s|^2 + 1) - \left( \frac{\lambda^* + \mu^*}{\sqrt{2}} \right)^2 s^2 - \left( \frac{\lambda + \mu}{\sqrt{2}} \right)^2 s^* \\
\left. \begin{aligned} \left( \frac{\Delta x}{x_0} \right)^2 &= \frac{|\lambda - \mu|^2}{2} \\ \left( \frac{\Delta p}{p_0} \right)^2 &= \frac{|\lambda + \mu|^2}{2} \end{aligned} \right\} \text{ (independent of } s)
\end{aligned}$$

We see that the (dimensionless) uncertainties in position and momentum are different, so are the energies. In the next section, we prove that for a squeezed state,  $\lambda$  and  $\mu$  must evolve as  $\lambda(t) = \lambda(0)e^{i\omega t} = \cosh(r)e^{i\omega t}$  and  $\mu(t) = \mu e^{-i\omega t} = \sinh(r)e^{i(\omega t - \phi)}$ , while  $s = |s|e^{i\theta}$  does not change.

Then, after some simplification, we get,

$$\left\{ \begin{aligned} \left\langle \frac{\hat{x}}{x_0} \right\rangle &= 2 \operatorname{Re} \left\{ \frac{\lambda(t) - \mu(t)}{\sqrt{2}} s^* \right\} = \sqrt{2}|s| [\cosh(r) \cos(\omega t - \theta) - \sinh(r) \sin(\omega t + \theta - \phi)] \\ \left\langle \frac{\hat{p}}{p_0} \right\rangle &= 2 \operatorname{Im} \left\{ \frac{\lambda(t)^* + \mu(t)^*}{\sqrt{2}} s \right\} = \sqrt{2}|s| [\cosh(r) \sin(\theta - \omega t) + \sinh(r) \sin(\omega t + \theta + \phi)] \\ \frac{(\Delta x)^2}{x_0^2} &= \frac{|\cosh(r)e^{i\omega t} - \sinh(r)e^{i(\phi - \omega t)}|^2}{2} = \frac{\cosh(2r) - \sinh(2r) \cos(2\omega t - \phi)}{2} \\ \frac{(\Delta p)^2}{p_0^2} &= \frac{|\cosh(r)e^{i\omega t} + \sinh(r)e^{i(\phi - \omega t)}|^2}{2} = \frac{\cosh(2r) + \sinh(2r) \cos(2\omega t - \phi)}{2} \end{aligned} \right. \quad (9)$$

We can solve  $\hat{Q}|s\rangle = s|s\rangle$  in position basis, and show that the wave function is a Gaussian peaked at  $\langle \hat{x} \rangle$  with standard deviation  $\Delta x$ , both of which are sinusoidal functions of time. When  $s = 0$ , the state is called squeezed vacuum, where the wave function is a Gaussian peaked at  $x = 0$ , but the standard deviation oscillates with time. For  $r = 0$ , the squeezed state reduces to the regular coherent state. When both  $r$  and  $s$  are 0, we get back the vacuum state  $|0\rangle$ .

### 2.2.1 Expansion of squeezed state in eigenstate basis and its time evolution

$$\begin{aligned}
\text{Let } |s\rangle &= \sum_{n=0}^{\infty} c_n |n\rangle. \text{ Then, } \hat{Q}|s\rangle = s|s\rangle \implies \hat{Q} \sum_{n=0}^{\infty} c_n |n\rangle = s \sum_{n=0}^{\infty} c_n |n\rangle \\
\implies \sum_{n=0}^{\infty} c_n \lambda \sqrt{n} |n-1\rangle + \mu \sqrt{n+1} |n+1\rangle &= s \sum_{n=0}^{\infty} c_n |n\rangle
\end{aligned}$$

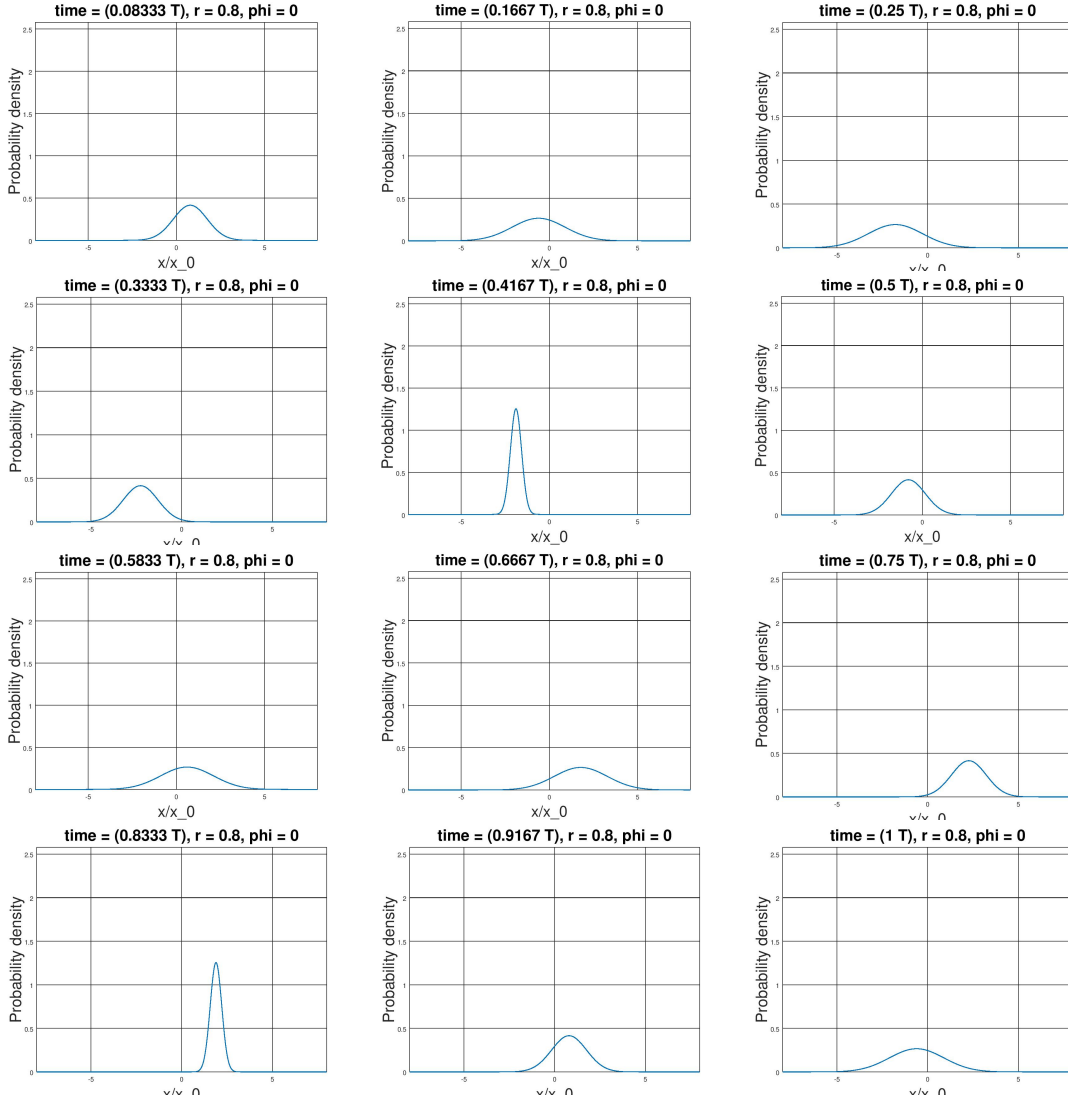


**Figure 2:** Time evolution of a squeezed coherent state with  $r = 0.8$  and  $s = 1$

$$\begin{aligned}
 \Rightarrow s \sum_{n=0}^{\infty} c_n |n\rangle &= \sum_{n=0}^{\infty} (c_{n+1} \lambda \sqrt{n+1} + c_{n-1} \mu \sqrt{n}) |n\rangle \\
 \Rightarrow s c_n &= \lambda \sqrt{n+1} c_{n+1} + \mu \sqrt{n} c_{n-1}
 \end{aligned} \tag{10}$$

We need to solve this recursion relation.

**Case  $s \neq 0$**

From (10),  $c_n = a \sqrt{n+1} c_{n+1} + b \sqrt{n} c_{n-1}$  (where  $a = \frac{\lambda}{s}$ ,  $b = \frac{\mu}{s}$ ). Let  $c_n = d_n \sqrt{n!}$  (see [11])

$$\Rightarrow d_n \sqrt{n!} = a d_{n+1} (n+1) \sqrt{n!} + b d_{n-1} \sqrt{n!}$$

$$\Rightarrow d_n = a d_{n+1} (n+1) + b d_{n-1}. \text{ Let } f(x) = \sum_{n=0}^{\infty} d_n x^n$$

$$\begin{aligned}
\Rightarrow f(x) &= a \sum_{n=0}^n d_{n+1}(n+1)x^n + b \sum_{n=0}^{\infty} d_{n-1}x^n \\
&= a \sum_{n=1}^{\infty} d_n n x^{n-1} + b x f(x) \\
&= a \sum_{n=0}^{\infty} n d_n x^{n-1} + b x f(x) \\
&= a x f'(x) + b x f(x) \\
\Rightarrow a f'(x) &= f(x)(1 - b x) \\
\Rightarrow \frac{f'(x)}{f(x)} &= \frac{1}{a} - \frac{b}{a} x \\
\Rightarrow f(x) &= C e^{\frac{x}{a} - \frac{b x^2}{2a}} \tag{11}
\end{aligned}$$

We know  $e^{2ty-y^2} = \sum_{n=0}^{\infty} H_n(t) \frac{y^n}{n!}$ , where  $H_n(t)$  is the Hermite polynomial of  $n$ th order [12].

Here in equation (11)  $y = x\sqrt{\frac{b}{2a}}$  and  $t = \frac{1}{\sqrt{2ab}}$ .

Therefore,  $e^{\frac{x}{a} - \frac{b x^2}{2a}} = \sum_{n=0}^{\infty} H_n\left(\frac{1}{\sqrt{2ab}}\right) \frac{x^n \left(\frac{b}{2a}\right)^{n/2}}{n!}$ , and

$$\begin{aligned}
c_n = d_n \sqrt{n!} &= \frac{H_n\left(\frac{1}{\sqrt{2ab}}\right) \left(\frac{b}{a}\right)^{n/2}}{\sqrt{2^n n!}} \\
&= \frac{H_n\left(\frac{s}{\sqrt{2\mu\lambda}}\right) \left(\frac{\mu}{\lambda}\right)^{n/2}}{\sqrt{2^n n!}}
\end{aligned}$$

$$\begin{aligned}
\text{Thus, } |s, t\rangle &= C \sum_{n=0}^{\infty} \frac{H_n\left(\frac{s}{\sqrt{2\mu\lambda}}\right) \left(\frac{\mu}{\lambda}\right)^{n/2}}{\sqrt{2^n n!}} e^{-i(n+\frac{1}{2})\omega t} |n, 0\rangle \quad (C \text{ is a normalization constant}) \\
&= C e^{-\frac{i\omega t}{2}} \sum_{n=0}^{\infty} \frac{H_n\left(\frac{s}{\sqrt{2(\mu e^{-i\omega t})(\lambda e^{i\omega t})}}\right) \left(\frac{\mu e^{-i\omega t}}{\lambda e^{i\omega t}}\right)^{n/2}}{\sqrt{2^n n!}} |n, 0\rangle
\end{aligned}$$

Therefore, the state evolves as if it remains a squeezed state with the same value of  $s$ , while  $\lambda$  and  $\mu$  evolve as  $\lambda e^{i\omega t}$  and  $\mu e^{-i\omega t}$ , respectively.

**Case**  $s = 0$ ,  $\mu \neq 0$ , squeezed vacuum

From (10), we get  $\lambda\sqrt{n+1}c_{n+1} + \mu\sqrt{n}c_{n-1} = 0$ .

Let  $e_n = c_n \sqrt{n!}$

$$\Rightarrow \lambda\sqrt{n+1} \frac{e_{n+1}}{\sqrt{(n+1)!}} + \mu\sqrt{n} \frac{e_{n-1}}{\sqrt{(n-1)!}} = 0$$

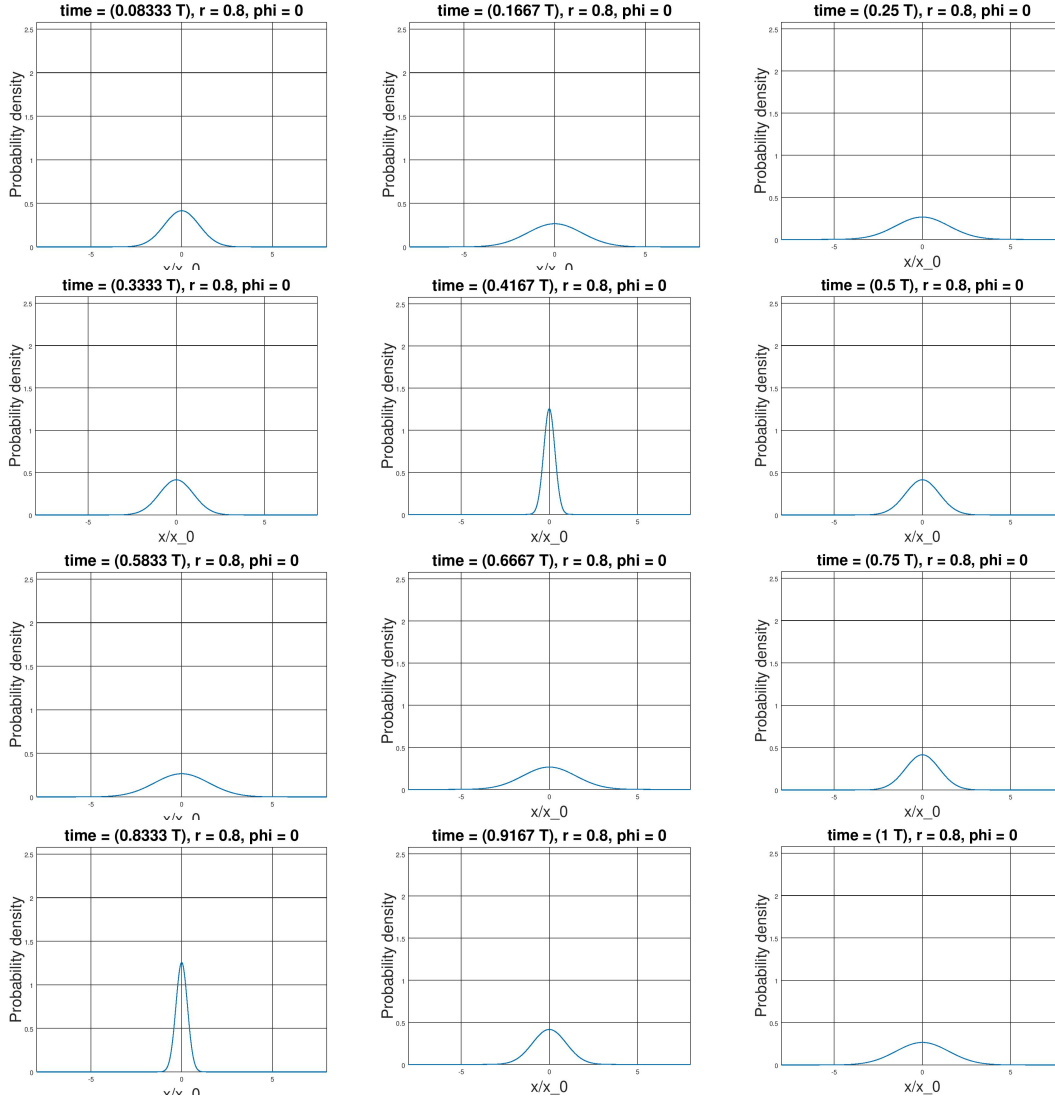


**Figure 3:** Time evolution of probability density of a squeezed vacuum state with  $r = 0.8$

$$\begin{aligned}
\Rightarrow e_{n+1} &= -\frac{\mu}{\lambda} n e_{n-1} \\
\Rightarrow e_{n+2} &= -\frac{\mu}{\lambda} (n+1) e_n \text{ (replacing } n \text{ with } n+1) \\
\Rightarrow \frac{e_{2n}}{e_0} &= \frac{e_{2n}}{e_{2n-2}} \frac{e_{2n-2}}{e_{2n-4}} \dots \frac{e_2}{e_0} \\
&= \left(-\frac{\mu}{\lambda}\right) (2n-1) \left(-\frac{\mu}{\lambda}\right) (2n-3) \dots \left(-\frac{\mu}{\lambda}\right) 1. \\
&= \left(-\frac{\mu}{\lambda}\right)^n \cdot (2n-1)(2n-3) \dots 1 \\
&= (-1)^n \left(\frac{\mu}{\lambda}\right)^n \frac{(2n)(2n-1) \dots 2 \cdot 1}{2^n \cdot n!} \\
&= (-1)^n \left(\frac{\mu}{\lambda}\right)^n \frac{(2n)!}{2^n \cdot n!}
\end{aligned}$$

$$\begin{aligned}
\text{Similarly, } \frac{e_{2n+1}}{e_1} &= \frac{e_{2n+1}}{e_{2n-1}} \frac{e_{2n-1}}{e_{2n-3}} \dots \frac{e_3}{e_1} \\
&= \left(-\frac{\mu}{\lambda}\right)^n \cdot (2n)(2n-2) \dots 2. \\
&= (-1)^n \left(\frac{\mu}{\lambda}\right)^n 2^n \cdot n!
\end{aligned}$$

By ratio test, it can be shown that  $\sum_{n=0}^{\infty} |c_{2n+1}|^2$  does not converge, and hence,  $c_1$  must be zero, making all other odd coefficients zero. Therefore, squeezed vacuum is only composed of even eigenstates of Hamiltonian.

## 2.3 Classical Brownian motion under harmonic potential

### 2.3.1 Langevin equation

It turns out that the motion of a classical particle undergoing Brownian motion can mimic a squeezed state, under special circumstances. The dynamics of a particle undergoing Brownian motion is governed by the Langevin equation,

$$m\ddot{x} = -\frac{dV(x)}{dx} - b\dot{x} + m\xi(t) \quad (12)$$

where  $-\frac{dV(x)}{dx}$  is the force acting on the particle due to potential  $V(x)$ ,  $-b\dot{x}$  is the effective frictional force acting on the particle due to viscosity of the medium, and  $\xi(t)$  is a time dependent stochastic force. For the Brownian motion of a particle in a normal heat bath of temperature  $T$ , the stochastic force is a white noise (see [13], [14]).  $\overline{\xi(t)} = 0$  and  $\overline{\xi(t_1)\xi(t_2)} = a\delta(t_1 - t_2)$ , where the overhead line denotes an average over the distribution of  $\xi(t)$ .

### 2.3.2 Explanation of the nature of correlation of the stochastic force

To see why this happens, we note that when  $t_1 \neq t_2$ , the two stochastic forces are uncorrelated, and the average of their product is zero. When the two times  $t_1$  and  $t_2$  are equal, the force acts like a Dirac delta function because the velocity of the Brownian particle changes instantaneously after being hit by a medium particle, implying that the change in momentum imparted by this instantaneous force is finite. Now we show that for  $a = \frac{2\gamma kT}{m}$ , where  $k$  is the Boltzmann's constant, and  $V(x) = 0$ , the velocity of the

Brownian particle tends to a thermal (Maxwell-Boltzmann) distribution with temperature  $T$ , at large times.

**Proof:** When  $V(x) = 0$ ,

$$m\dot{v} + m\gamma v = m\xi(t) \quad (13)$$

$$\begin{aligned} \implies e^{\gamma t}(\dot{v} + \gamma v) &= e^{\gamma t}\xi(t) \\ \implies \frac{d(v e^{\gamma t})}{dt} &= e^{\gamma t}\xi(t) \\ \implies v e^{\gamma t} - v(0) &= \int_0^t e^{\gamma s}\xi(s) ds \\ \implies v(t) &= v(0)e^{-\gamma t} + e^{-\gamma t} \int_0^t e^{\gamma s}\xi(s) ds \\ \implies v(t_1)v(t_2) &= v(0)^2 e^{-\gamma(t_1+t_2)} + v(0)a e^{-\gamma(t_1+t_2)} \left[ \int_0^{t_1} e^{\gamma s}\xi(s) ds + \int_0^{t_2} e^{\gamma s}\xi(s) ds \right] \\ &\quad + e^{-\gamma(t_1+t_2)} \int_0^{t_1} \int_0^{t_2} e^{\gamma(s_1+s_2)} \xi(s_1)\xi(s_2) ds_1 ds_2 \end{aligned}$$

Taking averages over the distribution,

$$\begin{aligned} \overline{v(t_1)v(t_2)} &= v(0)^2 e^{-\gamma(t_1+t_2)} + v(0)a e^{-\gamma(t_1+t_2)} \left[ \int_0^{t_1} e^{\gamma s} \overline{\xi(s)} ds + \int_0^{t_2} e^{\gamma s} \overline{\xi(s)} ds \right] \\ &\quad + e^{-\gamma(t_1+t_2)} \int_0^{t_1} \int_0^{t_2} e^{\gamma(s_1+s_2)} \overline{\xi(s_1)\xi(s_2)} ds_1 ds_2 \\ &= v(0)^2 e^{-\gamma(t_1+t_2)} + e^{-\gamma(t_1+t_2)} \int_0^{t_1} \int_0^{t_2} e^{\gamma(s_1+s_2)} a \delta(s_1 - s_2) ds_1 ds_2 \\ &= v(0)^2 e^{-\gamma(t_1+t_2)} + a e^{-\gamma(t_1+t_2)} \int_0^{\min(t_1, t_2)} e^{\gamma(2s_1)} a ds_1 \end{aligned}$$

Therefore,  $\overline{v(t)^2} = v(0)^2 e^{-2\gamma t} + a e^{-2\gamma t} \frac{e^{2\gamma t} - 1}{2\gamma}$ . When  $t \rightarrow \infty$ ,  $\overline{v(t)^2} = \frac{a}{2\gamma}$ . But, in thermal equilibrium,  $\frac{m\overline{v^2}}{2} = \frac{kT}{2} \implies \overline{v^2} = \frac{kT}{m}$ . Hence,  $a = \frac{2\gamma kT}{m}$ . To prove this, we could also Fourier transform the Langevin equation (13), solve it algebraically, and inverse transform it. This method is illustrated in the next section.

### 2.3.3 Fluctuation dissipation theorem and the claim

Using this value of  $a$  and this method, it can be proved that  $\frac{m\omega^2 \overline{x^2}}{2} = \frac{kT}{2}$  for a harmonic potential (see section 3 of chapter II in [15]). These results are known as “Fluctuation dissipation theorem”, which basically shows whatever may be the initial position and velocity of the particle, after long enough time random thermal fluctuations will make

each quadratic degree of freedom have energy  $\frac{kT}{2}$ , in average. This results also hold for random noise in LCR circuits, where the differential equation for the time evolution of the charge in the capacitor is identical to the equation of the displacement a damped harmonic oscillator.

It is claimed in the article by Klaers et. al [2] that a certain kind of stochastic force (see equation (14)) will lead to different variance (hence, different effective temperature) in position and momentum coordinates, as seen in a rotating frame.

### 3 Proof of the claim

Consider a particle in a Harmonic potential, undergoing Brownian motion for which

$$\xi(t) = a_0[e^{\tilde{r}}\xi_1(t)\cos(\omega t) + e^{-\tilde{r}}\xi_2(t)\sin(\omega t)] \quad (14)$$

where  $a_0^2 = \frac{2\gamma kT}{m}$ , and  $\xi_1(t)$  and  $\xi_2(t)$  are two independent, uncorrelated stochastic forces which satisfy  $\overline{\xi_i(t_1)\xi_j(t_2)} = \delta_{ij}\delta(t_1 - t_2)$ .  $\tilde{r}$  is a real number. Thus, the equations of motion are,

$$m\dot{x} = p \quad (15)$$

$$\dot{p} = -m\omega_0^2 x^2 - m\gamma\dot{x} + m\xi(t) \quad (16)$$

Recall that  $x_0 = \sqrt{\frac{\hbar}{m\omega_0}}$  and  $p_0 = \sqrt{\hbar m\omega_0}$ . We can write (15) and (16) in terms of dimensionless variables  $X = \frac{x}{x_0}$  and  $P = \frac{p}{p_0}$ , and then the equations become

$$\dot{X} = \omega_0 P \quad (17)$$

$$\dot{P} = -\omega_0 X - \frac{\gamma}{\omega_0} \dot{X} + \frac{m}{p_0} \xi(t) \quad (18)$$

Fourier transforming the above equations, we get,

$$-i\omega \tilde{X}(\omega) = \omega_0 \tilde{P}(\omega) \quad (19)$$

$$-i\omega \tilde{P}(\omega) = -\omega_0 \tilde{X}(\omega) + i\frac{\gamma}{\omega_0} \tilde{X}(\omega) + \frac{m}{p_0} \tilde{\xi}(\omega) \quad (20)$$

Note that in this article,

$$\begin{aligned} f(t) &= \frac{1}{\sqrt{2\pi}} \int_{-\infty}^{\infty} \tilde{f}(\omega) e^{-i\omega t} d\omega \\ \tilde{f}(\omega) &= \frac{1}{\sqrt{2\pi}} \int_{-\infty}^{\infty} f(t) e^{i\omega t} dt \end{aligned}$$



### 3.0.1 Preliminaries

Let us introduce the notation  $\int_y f(y)$  to denote  $\int_{-\infty}^{\infty} f(y) dy$ .

$$\begin{aligned} \text{We know } \overline{\xi_1(t_1)\xi_1(t_2)} &= \delta(t_1 - t_2). \text{ Then, } \overline{\widetilde{\xi_1}(\omega_1)\widetilde{\xi_1}(\omega_2)} = \frac{1}{2\pi} \int_{t_1} \int_{t_2} \overline{\xi_1(t_1)\xi_1(t_2)} e^{i\omega_1 t_1} e^{i\omega_2 t_2} \\ &= \frac{1}{2\pi} \int_{t_1} \int_{t_2} \delta(t_1 - t_2) e^{i\omega_1 t_1} e^{i\omega_2 t_2} \\ &= \frac{1}{2\pi} \int_{t_1} e^{i\omega_1 t_1} e^{i\omega_2 t_1} \\ &= \delta(\omega_1 + \omega_2) \end{aligned}$$

Therefore,

$$\overline{\widetilde{\xi_i}(\omega_1)\widetilde{\xi_j}(\omega_2)} = \delta_{ij}\delta(\omega_1 + \omega_2) \quad (21)$$

We also make use of the following integrals (valid when  $\omega_D^2 = \omega_0^2 - \frac{\gamma^2}{4} > 0$ , i.e. an underdamped oscillator)

$$I_1(\omega_0, \gamma) = \int_{\omega} \frac{1}{(\omega_0^2 - \omega^2)^2 + \omega^2 \gamma^2} = \frac{\pi}{\omega_0^2 \gamma} \quad (22)$$

$$I_2(\omega_0, \gamma) = \int_{\omega} \frac{\omega^2}{(\omega_0^2 - \omega^2)^2 + \omega^2 \gamma^2} = \frac{\pi}{\gamma} \quad (23)$$

$$I_3(\omega_0, \gamma) = \int_{\omega} \frac{1}{(\omega_0^2 - \omega^2 - i\omega\gamma)[(\omega_0^2 - (\omega + 2\omega_0)^2 + i(\omega + 2\omega_0)\gamma)]} = \frac{-\pi(\omega_0 + \frac{i\gamma}{2})}{2\gamma\omega_0(\omega_0^2 + \frac{\gamma^2}{4})} \quad (24)$$

$$I_4(\omega_0, \gamma) = \int_{\omega} \frac{\omega}{(\omega_0^2 - \omega^2 - i\omega\gamma)[(\omega_0^2 - (\omega + 2\omega_0)^2 + i(\omega + 2\omega_0)\gamma)]} = \frac{\pi(\omega_0 + \frac{i\gamma}{2})}{2\gamma(\omega_0^2 + \frac{\gamma^2}{4})} \quad (25)$$

$$\begin{aligned} I_5(\omega_0, \gamma) &= \int_{\omega} \frac{\omega(\omega + 2\omega_0)}{(\omega_0^2 - \omega^2 - i\omega\gamma)[(\omega_0^2 - (\omega + 2\omega_0)^2 + i(\omega + 2\omega_0)\gamma)]} = \frac{\pi}{2\gamma} + \frac{\pi(-\frac{i\gamma}{2})(\omega_0 + \frac{i\gamma}{2})}{2\gamma(\omega_0^2 + \frac{\gamma^2}{4})} \\ &= \frac{\pi(\omega_0^2 + \frac{\gamma^2}{2} - \frac{i\gamma\omega_0}{2})}{2\gamma(\omega_0^2 + \frac{\gamma^2}{4})} \end{aligned} \quad (26)$$

These can be proved using contour integration. If  $f(t)$  is a function of  $t$  having a Fourier transform  $\widetilde{f}(\omega)$ , then, the Fourier transform of the function  $f(t) \cos(\omega_0 t)$  is,  $\frac{1}{2\pi} \int_t f(t) \cos(\omega_0 t) e^{i\omega t} = \frac{1}{2\pi} \int_t f(t) \frac{e^{i(\omega+\omega_0)t} + e^{i(\omega-\omega_0)t}}{2} = \frac{\widetilde{f}(\omega + \omega_0) + \widetilde{f}(\omega - \omega_0)}{2}$ . Similarly, the Fourier transform of  $f(t) \sin(\omega_0 t)$  is  $\frac{\widetilde{f}(\omega + \omega_0) - \widetilde{f}(\omega - \omega_0)}{2i}$ .

Then, from (14),

$$\tilde{\xi}(\omega) = \frac{a_0}{2} [e^{\tilde{r}} \tilde{\xi}_1(\omega + \omega_1) + e^{\tilde{r}} \tilde{\xi}_1(\omega - \omega_1) - ie^{-\tilde{r}} \tilde{\xi}_2(\omega + \omega_1) + ie^{-\tilde{r}} \tilde{\xi}_2(\omega - \omega_1)] \quad (27)$$

$$\begin{aligned} \text{Therefore, } \overline{\tilde{\xi}(\omega_1) \tilde{\xi}(\omega_2)} &= \frac{a_0^2}{4} \left[ e^{2r} \overline{\left\{ \tilde{\xi}_1(\omega_1 + \omega_0) + \tilde{\xi}_1(\omega_1 - \omega_0) \right\} \left\{ \tilde{\xi}_1(\omega_2 + \omega_0) + \tilde{\xi}_1(\omega_2 - \omega_0) \right\}} \right] \\ &\quad - \frac{a_0^2}{4} \left[ e^{-2r} \overline{\left\{ \tilde{\xi}_2(\omega_1 + \omega_0) + \tilde{\xi}_2(\omega_1 - \omega_0) \right\} \left\{ \tilde{\xi}_2(\omega_2 + \omega_0) + \tilde{\xi}_2(\omega_2 - \omega_0) \right\}} \right] \\ &\quad (\text{since cross terms are 0 in average}) \\ &= \frac{a_0^2}{4} [e^{2r} \{ \delta(\omega_1 + \omega_2 + 2\omega_0) + 2\delta(\omega_1 + \omega_2) + \delta(\omega_1 + \omega_2 - 2\omega_0) \}] \\ &\quad - \frac{a_0^2}{4} [e^{-2r} \{ \delta(\omega_1 + \omega_2 + 2\omega_0) + 2\delta(\omega_1 + \omega_2) + \delta(\omega_1 + \omega_2 - 2\omega_0) \}] \\ &= \frac{a_0^2}{2} [\sinh(2\tilde{r}) \{ \delta(\omega_1 + \omega_2 + 2\omega_0) + \delta(\omega_1 + \omega_2 - 2\omega_0) \} + 2 \cosh(2\tilde{r}) \delta(\omega_1 + \omega_2)] \end{aligned} \quad (28)$$

### 3.0.2 Calculation of Fourier transformed position and momentum

From (19) and (20),

$$\tilde{X}(\omega) = \frac{m\omega_0}{p_0} \frac{\tilde{\xi}(\omega)}{\omega_0^2 - \omega^2 - i\omega\gamma} \quad (29)$$

$$\tilde{P}(\omega) = -i \frac{m\omega}{p_0} \frac{\tilde{\xi}(\omega)}{\omega_0^2 - \omega^2 - i\omega\gamma} \quad (30)$$

Using (28), (29), and (30), we get the following results.

$$\begin{aligned} \overline{\tilde{X}(\omega_1) \tilde{X}(\omega_2)} &= \left( \frac{m\omega_0}{p_0} \right)^2 \frac{\overline{\tilde{\xi}(\omega_1) \tilde{\xi}(\omega_2)}}{(\omega_0^2 - \omega_1^2 - i\omega_1\gamma)(\omega_0^2 - \omega_2^2 - i\omega_2\gamma)} \\ &= \frac{1}{2} \left( \frac{m\omega_0 a_0}{p_0} \right)^2 \frac{[\sinh(2\tilde{r}) \{ \delta(\omega_1 + \omega_2 + 2\omega_0) + \delta(\omega_1 + \omega_2 - 2\omega_0) \} + 2 \cosh(2\tilde{r}) \delta(\omega_1 + \omega_2)]}{(\omega_0^2 - \omega_1^2 - i\omega_1\gamma)(\omega_0^2 - \omega_2^2 - i\omega_2\gamma)} \end{aligned} \quad (31)$$

$$\begin{aligned} \overline{\tilde{X}(\omega_1) \tilde{P}(\omega_2)} &= \frac{-i\omega_2}{2\omega_0} \left( \frac{m\omega_0 a_0}{p_0} \right)^2 \\ &\quad \times \frac{[\sinh(2\tilde{r}) \{ \delta(\omega_1 + \omega_2 + 2\omega_0) + \delta(\omega_1 + \omega_2 - 2\omega_0) \} + 2 \cosh(2\tilde{r}) \delta(\omega_1 + \omega_2)]}{(\omega_0^2 - \omega_1^2 - i\omega_1\gamma)(\omega_0^2 - \omega_2^2 - i\omega_2\gamma)} \end{aligned} \quad (32)$$

$$\begin{aligned} \overline{\tilde{P}(\omega_1) \tilde{P}(\omega_2)} &= -\frac{1}{2} \frac{\omega_1 \omega_2}{\omega_0^2} \left( \frac{m\omega_0 a_0}{p_0} \right)^2 \\ &\quad \times \frac{[\sinh(2\tilde{r}) \{ \delta(\omega_1 + \omega_2 + 2\omega_0) + \delta(\omega_1 + \omega_2 - 2\omega_0) \} + 2 \cosh(2\tilde{r}) \delta(\omega_1 + \omega_2)]}{(\omega_0^2 - \omega_1^2 - i\omega_1\gamma)(\omega_0^2 - \omega_2^2 - i\omega_2\gamma)} \end{aligned} \quad (33)$$

### 3.1 Calculation of variance in position

We inverse tranform (31) to time domain, to get the variance of position, averaged over the distribution of the stochastic force. We also note that the average position is zero, as the average stochastic force is zero (hence, its fourier transform is zero, hence from (29), average of Fourier transform of position is zero, from which this result follows).

$$\begin{aligned}
\overline{X^2(t)} &= \frac{1}{2\pi} \int_{\omega_1} \int_{\omega_2} \overline{\tilde{X}(\omega_1) \tilde{X}(\omega_2)} e^{-i\omega_1 t} e^{-i\omega_2 t} \\
&= \frac{1}{4\pi} \left( \frac{m\omega_0 a_0}{p_0} \right)^2 \left[ 2 \cosh(2\tilde{r}) \int_{\omega_1} \frac{1}{(\omega_0^2 - \omega_1^2)^2 + \omega_1^2 \gamma^2} \right] \\
&\quad + \frac{1}{4\pi} \left( \frac{m\omega_0 a_0}{p_0} \right)^2 \left[ \sinh(2\tilde{r}) \int_{\omega_1} \frac{e^{2i\omega_0 t}}{(\omega_0^2 - \omega_1^2 - i\omega_1 \gamma)[(\omega_0^2 - (\omega_1 + 2\omega_0)^2 + i(\omega_1 + 2\omega_0)\gamma)]} \right] \\
&\quad + \frac{1}{4\pi} \left( \frac{m\omega_0 a_0}{p_0} \right)^2 \left[ \sinh(2\tilde{r}) \int_{\omega_1} \frac{e^{-2i\omega_0 t}}{(\omega_0^2 - \omega_1^2 - i\omega_1 \gamma)[(\omega_0^2 - (\omega_1 - 2\omega_0)^2 + i(\omega_1 - 2\omega_0)\gamma)]} \right] \\
&= \frac{1}{4\pi} \left( \frac{m\omega_0 a_0}{p_0} \right)^2 \left[ 2 \cosh(2\tilde{r}) I_1(\omega_0, \gamma) + \sinh(2\tilde{r}) \{ e^{2i\omega_0 t} I_3(\omega_0, \gamma) + e^{-2i\omega_0 t} I_3(-\omega_0, \gamma) \} \right] \\
e^{2i\omega_0 t} I_3(\omega_0, \gamma) + e^{-2i\omega_0 t} I_3(-\omega_0, \gamma) &= \frac{-\pi}{2\gamma(\omega_0^2 + \frac{\gamma^2}{4})} \left\{ \left( 1 + \frac{i\gamma}{2\omega_0} \right) e^{2i\omega_0 t} + \left( 1 - \frac{i\gamma}{\gamma\omega_0} \right) e^{-2i\omega_0 t} \right\} \\
&= \frac{-\pi}{2\gamma(\omega_0^2 + \frac{\gamma^2}{4})} \left\{ 2 \cos(2\omega_0 t) + \frac{i\gamma}{2\omega_0} 2i \sin(2\omega_0 t) \right\} \\
&= \frac{-\pi}{\gamma(\omega_0^2 + \frac{\gamma^2}{4})} \left\{ \cos(2\omega_0 t) - \frac{\gamma}{2\omega_0} \sin(2\omega_0 t) \right\}
\end{aligned}$$

Substituting this expression in the expression of variance in position, we get,

$$\begin{aligned}
\overline{X^2(t)} &= \frac{1}{4\pi} \left( \frac{m\omega_0 a_0}{p_0} \right)^2 \left[ 2 \cosh(2\tilde{r}) \frac{\pi}{\omega_0^2 \gamma} - \frac{\pi \sinh(2\tilde{r})}{\omega_0^2 + \frac{\gamma^2}{4}} \left\{ \cos(2\omega_0 t) - \frac{\gamma}{2\omega_0} \sin(2\omega_0 t) \right\} \right] \\
&= \frac{1}{4\pi} \frac{m^2 \omega_0^2}{m \hbar \omega_0} \frac{\pi}{\omega_0^2 \gamma} \frac{2\gamma kT}{m} \left[ 2 \cosh(2\tilde{r}) - \frac{\sinh(2\tilde{r})}{1 + \frac{\gamma^2}{4\omega_0^2}} \left\{ \cos(2\omega_0 t) - \frac{\gamma}{2\omega_0} \sin(2\omega_0 t) \right\} \right] \\
&= \frac{kT}{2\hbar\omega_0} \left[ 2 \cosh(2\tilde{r}) - \frac{\sinh(2\tilde{r})}{1 + \frac{\gamma^2}{4\omega_0^2}} \left\{ \cos(2\omega_0 t) - \frac{\gamma}{2\omega_0} \sin(2\omega_0 t) \right\} \right]
\end{aligned} \tag{34}$$

### 3.2 Calculation of covariance in position and momentum

Similarly, we inverse transform the covariance of position and momentum to time domain.

$$\begin{aligned}
\overline{X(t)P(t)} &= \frac{1}{2\pi} \int_{\omega_1} \int_{\omega_2} \overline{\widetilde{X}(\omega_1)\widetilde{P}(\omega_2)} e^{-i\omega_1 t} e^{-i\omega_2 t} \\
&= \frac{-i}{4\pi\omega_0} \left( \frac{m\omega_0 a_0}{p_0} \right)^2 \left[ 2 \cosh(2\tilde{r}) \int_{\omega_1} \frac{\omega_1}{(\omega_0^2 - \omega_1^2)^2 + \omega_1^2 \gamma^2} \right] (= 0, \text{ as integrand is odd function}) \\
&+ \frac{-i}{4\pi\omega_0} \left( \frac{m\omega_0 a_0}{p_0} \right)^2 \left[ \sinh(2\tilde{r}) \int_{\omega_1} \int_{\omega_2} \frac{\omega_2 e^{-i(\omega_1 + \omega_2)t} \{ \delta(\omega_1 + \omega_2 + 2\omega_0) + \delta(\omega_1 + \omega_2 - 2\omega_0) \}}{(\omega_0^2 - \omega_1^2 - i\omega_1 \gamma)[(\omega_0^2 - (\omega_1 + 2\omega_0)^2 + i(\omega_1 + 2\omega_0)\gamma)]} \right] \\
&= \frac{-i\gamma kT}{2\pi\hbar} \sinh(2\tilde{r}) \left[ \int_{\omega_1} \frac{\omega_1 e^{2i\omega_0 t}}{(\omega_0^2 - \omega_1^2 - i\omega_1 \gamma)[(\omega_0^2 - (\omega_1 + 2\omega_0)^2 + i(\omega_1 + 2\omega_0)\gamma)]} \right] \\
&+ \frac{-i\gamma kT}{2\pi\hbar} \sinh(2\tilde{r}) \left[ \int_{\omega_1} \frac{\omega_1 e^{-2i\omega_0 t}}{(\omega_0^2 - \omega_1^2 - i\omega_1 \gamma)[(\omega_0^2 - (\omega_1 - 2\omega_0)^2 + i(\omega_1 - 2\omega_0)\gamma)]} \right] \\
&= \frac{-i\gamma kT}{2\pi\hbar} \sinh(2\tilde{r}) [I_4(\omega_0, \gamma) e^{2i\omega_0 t} + I_4(-\omega_0, \gamma) e^{-2i\omega_0 t}] \\
I_4(\omega_0, \gamma) e^{2i\omega_0 t} + I_4(-\omega_0, \gamma) e^{-2i\omega_0 t} &= \frac{\pi}{2\gamma(\omega_0^2 + \frac{\gamma^2}{4})} \left[ \omega_0 e^{2i\omega_0 t} - \omega_0 e^{-2i\omega_0 t} + \frac{i\gamma}{2} (e^{2i\omega_0 t} + e^{-2i\omega_0 t}) \right] \\
&= \frac{i\pi}{\gamma(\omega_0^2 + \frac{\gamma^2}{4})} \left[ \omega_0 \sin(2\omega_0 t) + \frac{\gamma}{2} \cos(2\omega_0 t) \right]
\end{aligned}$$

$$\begin{aligned}
\text{Thus, } \overline{X(t)P(t)} &= \frac{-i\gamma kT}{2\pi\hbar} \sinh(2\tilde{r}) \frac{i\pi}{\gamma(\omega_0^2 + \frac{\gamma^2}{4})} \left[ \omega_0 \sin(2\omega_0 t) + \frac{\gamma}{2} \cos(2\omega_0 t) \right] \\
&= \frac{kT}{2\hbar\omega_0} \frac{\sinh(2\tilde{r})}{(1 + \frac{\gamma^2}{4\omega_0^2})} \left[ \sin(2\omega_0 t) + \frac{\gamma}{2\omega_0} \cos(2\omega_0 t) \right] \tag{35}
\end{aligned}$$

### 3.3 Calculation of variance in momentum

$$\begin{aligned}
\overline{P^2(t)} &= \frac{1}{2\pi} \int_{\omega_1} \int_{\omega_2} \overline{\widetilde{P}(\omega_1)\widetilde{P}(\omega_2)} e^{-i\omega_1 t} e^{-i\omega_2 t} \\
&= -\frac{1}{4\pi} \left( \frac{ma_0}{p_0} \right)^2 \left[ 2 \cosh(2\tilde{r}) \int_{\omega_1} \frac{-\omega_1^2}{(\omega_0^2 - \omega_1^2)^2 + \omega_1^2 \gamma^2} \right] \\
&- \frac{1}{4\pi} \left( \frac{ma_0}{p_0} \right)^2 \left[ \sinh(2\tilde{r}) \int_{\omega_1} \frac{\omega_1(-2\omega_0 - \omega_1) e^{2i\omega_0 t}}{(\omega_0^2 - \omega_1^2 - i\omega_1 \gamma)[(\omega_0^2 - (\omega_1 + 2\omega_0)^2 + i(\omega_1 + 2\omega_0)\gamma)]} \right] \\
&- \frac{1}{4\pi} \left( \frac{ma_0}{p_0} \right)^2 \left[ \sinh(2\tilde{r}) \int_{\omega_1} \frac{\omega_1(2\omega_0 - \omega_1) e^{-2i\omega_0 t}}{(\omega_0^2 - \omega_1^2 - i\omega_1 \gamma)[(\omega_0^2 - (\omega_1 - 2\omega_0)^2 + i(\omega_1 - 2\omega_0)\gamma)]} \right] \\
&= \frac{1}{4\pi} \left( \frac{ma_0}{p_0} \right)^2 [2 \cosh(2\tilde{r}) I_2(\omega_0, \gamma) + \sinh(2\tilde{r}) \{ I_5(\omega_0, \gamma) e^{2i\omega_0 t} + I_5(-\omega_0, \gamma) e^{-2i\omega_0 t} \}] \\
&= \frac{1}{4\pi} \left( \frac{2\gamma kT}{\hbar\omega_0} \right) [2 \cosh(2\tilde{r}) I_2(\omega_0, \gamma) + \sinh(2\tilde{r}) \{ I_5(\omega_0, \gamma) e^{2i\omega_0 t} + I_5(-\omega_0, \gamma) e^{-2i\omega_0 t} \}]
\end{aligned}$$

$$\begin{aligned}
I_5(\omega_0, \gamma)e^{2i\omega_0 t} + I_5(-\omega_0, \gamma)e^{-2i\omega_0 t} \\
= \frac{\pi}{2\gamma\left(\omega_0^2 + \frac{\gamma^2}{4}\right)} \left[ 2\left(\omega_0^2 + \frac{\gamma^2}{2}\right) \cos(2\omega_0 t) - \frac{i\gamma}{2}\omega_0 e^{2i\omega_0 t} + \frac{i\gamma}{2}\omega_0 e^{-2i\omega_0 t} \right] \\
= \frac{\pi}{\gamma\left(\omega_0^2 + \frac{\gamma^2}{4}\right)} \left[ \left(\omega_0^2 + \frac{\gamma^2}{2}\right) \cos(2\omega_0 t) + \frac{\gamma\omega_0}{2} \sin(2\omega_0 t) \right]
\end{aligned}$$

$$\begin{aligned}
\text{Thus, } \overline{P^2(t)} &= \frac{1}{4\pi} \frac{\pi}{\gamma} \frac{2\gamma kT}{\hbar\omega_0} \left[ 2 \cosh(2\tilde{r}) + \frac{\sinh(2\tilde{r})}{1 + \frac{\gamma^2}{4\omega_0^2}} \left\{ \left(1 + \frac{\gamma^2}{2\omega_0^2}\right) \cos(2\omega_0 t) + \frac{\gamma}{2\omega_0} \sin(2\omega_0 t) \right\} \right] \\
&= \frac{kT}{2\hbar\omega_0} \left[ 2 \cosh(2\tilde{r}) + \frac{\sinh(2\tilde{r})}{1 + \frac{\gamma^2}{4\omega_0^2}} \left\{ \left(1 + \frac{\gamma^2}{2\omega_0^2}\right) \cos(2\omega_0 t) + \frac{\gamma}{2\omega_0} \sin(2\omega_0 t) \right\} \right] \quad (36)
\end{aligned}$$

### 3.4 Rotating coordinates

Let us define “rotating coordinates”,

$$\begin{aligned}
X_1 &= X \cos(\omega_0 t) - P \sin(\omega_0 t) \\
X_2 &= X \sin(\omega_0 t) + P \cos(\omega_0 t)
\end{aligned} \quad (37)$$

Therefore,  $X_1^2 = X^2 \cos^2(\omega_0 t) + P^2 \sin^2(\omega_0 t) - 2XP \sin(\omega_0 t) \cos(\omega_0 t)$

$$\Rightarrow X_1^2 = \frac{X^2}{2} + \frac{P^2}{2} + \frac{X^2}{2} \cos(2\omega_0 t) - \frac{P^2}{2} \cos(2\omega_0 t) - XP \sin(2\omega_0 t) \quad (38)$$

Similarly,

$$X_2^2 = \frac{X^2}{2} + \frac{P^2}{2} - \frac{X^2}{2} \cos(2\omega_0 t) + \frac{P^2}{2} \cos(2\omega_0 t) + XP \sin(2\omega_0 t) \quad (39)$$

Now we use the fact that over a long time  $t(\gg \frac{1}{\omega_0})$ ,  $\langle \sin(n\omega_0 t) \rangle = \langle \cos(n\omega_0 t) \rangle = 0$ ,

and  $\langle \sin^2(n\omega_0 t) \rangle = \langle \cos^2(n\omega_0 t) \rangle = \frac{1}{2}$ , where  $\langle f(t) \rangle = \frac{\int_0^t f(s) ds}{t}$ , the time averaged value of  $f(t)$ .

Using (34), (35), (36) and (38), we get,

$$\begin{aligned}
\langle \overline{X_1^2} \rangle &= \frac{kT}{4\hbar\omega_0} \left[ 4 \cosh(2\tilde{r}) - \frac{\sinh(2\tilde{r})}{1 + \frac{\gamma^2}{4\omega_0^2}} \cdot \frac{1}{2} - \frac{\sinh(2\tilde{r})}{1 + \frac{\gamma^2}{4\omega_0^2}} \cdot \frac{1}{2} \cdot \left( 1 + \frac{\gamma^2}{2\omega_0^2} \right) - \frac{\sinh(2\tilde{r})}{1 + \frac{\gamma^2}{4\omega_0^2}} \cdot \frac{1}{2} \cdot 2 \right] \\
&= \frac{kT}{4\hbar\omega_0} \left[ 4 \cosh(2\tilde{r}) - 2 \frac{\sinh(2\tilde{r})}{1 + \frac{\gamma^2}{4\omega_0^2}} \left( 1 + \frac{\gamma^2}{8\omega_0^2} \right) \right] \\
&\approx \frac{kT}{\hbar\omega_0} \left[ \cosh(2\tilde{r}) - \frac{\sinh(2\tilde{r})}{2} \right] \left( \text{in the limit of low damping, i.e. } \frac{\gamma}{\omega_0} \ll 1 \right)
\end{aligned}$$

Similarly, using (34), (35), (36) and (39), we get,

$$\begin{aligned}
\langle \overline{X_2^2} \rangle &= \frac{kT}{4\hbar\omega_0} \left[ 4 \cosh(2\tilde{r}) + \frac{\sinh(2\tilde{r})}{1 + \frac{\gamma^2}{4\omega_0^2}} \cdot \frac{1}{2} \cdot \left( 1 + \frac{\gamma^2}{2\omega_0^2} \right) + \frac{\sinh(2\tilde{r})}{1 + \frac{\gamma^2}{4\omega_0^2}} \cdot \frac{1}{2} + \frac{\sinh(2\tilde{r})}{1 + \frac{\gamma^2}{4\omega_0^2}} \cdot \frac{1}{2} \cdot 2 \right] \\
&= \frac{kT}{4\hbar\omega_0} \left[ 4 \cosh(2\tilde{r}) + 2 \frac{\sinh(2\tilde{r})}{1 + \frac{\gamma^2}{4\omega_0^2}} \left( 1 + \frac{\gamma^2}{8\omega_0^2} \right) \right] \\
&\approx \frac{kT}{\hbar\omega_0} \left[ \cosh(2\tilde{r}) + \frac{\sinh(2\tilde{r})}{2} \right] \left( \text{in the limit of low damping, i.e. } \frac{\gamma}{\omega_0} \ll 1 \right)
\end{aligned}$$

From (1), the energy in a quadratic degree of freedom  $X$  is,  $\frac{\hbar\omega_0}{2} \langle \overline{X^2} \rangle = \frac{kT^*}{2}$ , where  $T^*$  is the effective temperature.

Therefore, the effective temperatures in the two rotating coordinates are,

$$\begin{aligned}
T_{1}^* &= T \left[ \cosh(2\tilde{r}) - \frac{\sinh(2\tilde{r})}{2} \right] \\
T_{2}^* &= T \left[ \cosh(2\tilde{r}) + \frac{\sinh(2\tilde{r})}{2} \right]
\end{aligned} \tag{40}$$

where  $T$  is the temperature of the heat bath to which the harmonic oscillator is coupled and  $\tilde{r}$  is the parameter in the stochastic force (14). Note that the time-averaged energies in the non-rotating coordinates  $X(t)$  (potential energy) and  $P(t)$  (kinetic energy) are equal.

**Note:** It is claimed in [2], the stochastic force  $\xi(t) = a_0[e^{\tilde{r}}\xi_1(t)\cos(\omega t) + e^{-\tilde{r}}\xi_2(t)\sin(\omega t)]$  gives rise to effective temperatures  $T_{1,2}^* = Te^{\pm 2\tilde{r}}$ . The relation between  $r$  and  $\tilde{r}$  is not mentioned. This can be explained if the relation  $e^{4r} = \frac{\cosh(2\tilde{r}) - \frac{\sinh(2\tilde{r})}{2}}{\cosh(2\tilde{r}) + \frac{\sinh(2\tilde{r})}{2}}$ , i.e.  $r =$

$\frac{1}{4} \ln \left( \frac{e^{\tilde{r}} + 3}{3e^{4\tilde{r}} + 1} \right)$  is satisfied.

## 4 Other methods to get this result

### 4.1 Directly integrating the equations in Mathematica

We can write (15) and (16) in matrix form, and diagonalize the matrices to formally solve for  $x(t)$  and  $v(t)$  in terms of  $\xi(t)$ . Then we can calculate of  $\overline{x(t_1)x(t_2)}$ ,  $\overline{x(t_1)v(t_2)}$ , and  $\overline{v(t_1)v(t_2)}$  just like in subsection 2.3.2, and find the variance of the rotating coordinates. I did this calculation in Mathematica and got the same results as in section 3.4, under the limit of low damping.

### 4.2 Verification using a simulation

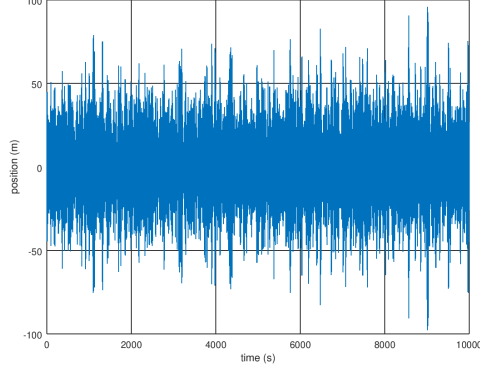
I created a C program [16] to numerically solve (12) and (14) with Runge-Kutta method [17] of order 4. The delta function force is simulated with a random force of very high magnitude (high compared to the spring force). The following graphs show that the energy in rotating coordinates are different. It is found that their ratio is close to the ratio obtained in (40).

## 5 How the Heat Engine works

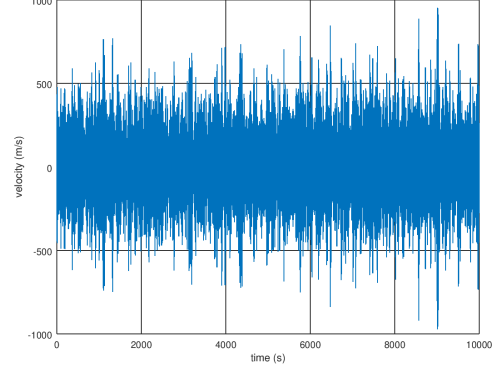
The working principle of the squeezed harmonic oscillator used in [2] is hereby explained. More details can be found in the supplement material [18] of their paper. They have created a nano beam structure made of GaAs that is doubly clamped, and allowed to vibrate. The nano-beam contains two doped layers, where a DC bias voltage can be applied to change the frequency of oscillation of the beam.

### 5.1 How the force is applied

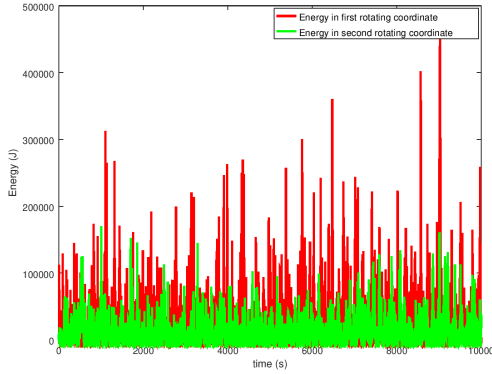
Due to the piezo-electric nature of GaAs, when an AC electric field is applied to it, it experiences a mechanical force, and oscillates according to it. The oscillator is weakly damped (Q factor is approximately  $10^3$ ). Now, an electric field of the form (14) is used, so that



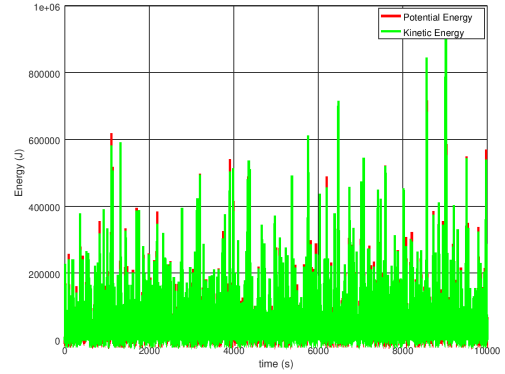
(a) position as a function of time



(b) velocity as a function of time



(c) energies in the two rotating coordinates as a function of time



(d) The average energy in position and momentum are almost equal.

**Figure 4:** A simulation of a Brownian harmonic oscillator under the stochastic force with  $a_0 = 1000, \tilde{r} = -0.4$ . In this, mass is taken to be unity. Note that the energy in rotating coordinates are different, while they are almost equal in the non-rotating coordinates, which can be justified by time averaging equations (34) and (36)

the beam experiences a similar mechanical force, and its displacement from equilibrium is described by the Langevin equation (12), where the force is given by (14).

## 5.2 How the quantities are measured

The displacement of the nano-beam is measured using Mach-Zehnder interferometry, where the path length of a laser beam changes as the nano-beam oscillates, creating a shift in the position of fringes, which can be used to calculate the displacement of the nano-beam. From the displacement, rotating coordinate amplitudes, their effective



temperatures, and all other quantities of interest can be found.

### 5.3 How it is used as a heat engine

The frequency of oscillation of the beam can be changed by altering the DC bias voltage. It has been shown in the supplement material [18] of that paper that the entropy in the two quadratures of the oscillator can be expressed as  $S_{1,2} = \frac{k_B}{2} \ln\left(\frac{k_B T_{1,2}}{\hbar\omega}\right) + \text{constant}$  (Where  $T_{1,2} = Te^{\pm 2r}$  are effective temperatures in the two rotating coordinates. Note that the absolute constant in entropy does not matter). The volume of the system is defined to be  $V = \frac{1}{\omega}$ , and it can be shown that internal energy  $U(S_1, S_2, V) = \frac{\hbar}{2V} \left( \exp\left(2\frac{S_1}{k_B} - 1\right) + \exp\left(2\frac{S_2}{k_B} - 1\right) \right)$ . Then, we can define pressure  $p = -\left(\frac{\partial U}{\partial V}\right)_{S_1, S_2} = \frac{k_B}{2} \frac{(T_1 + T_2)}{V}$ .

Now, the temperature  $T$  and squeezing parameter  $r$  can be varied by tweaking the stochastic force. This way, the oscillator is made to undergo an Otto cycle [1]. The adiabatic strokes of the Otto cycle are replaced by an isoentropic stroke, where the ratio  $\frac{T}{\omega}$  is kept constant (note that entropy is a function of  $\frac{k_B T}{\hbar\omega}$ ).

The natural frequency of the oscillator is in the order of MHz, whereas the cycle time of the Otto cycle is of several seconds. So, we can use the time average values for sines and cosines (and their squares, as in subsection 3.4), and assume that the rotating coordinates have a Gaussian distribution with mean zero, and variance proportional to  $T_1^*$  and  $T_2^*$ .

When the temperature is highest ( $T_h = 10000K$ ), the squeezing parameter is kept at a value  $r_h = 0.4$ , and when the temperature is lowest ( $T_c = 9500K$ ), the squeezing parameter is made zero. So, the effective highest temperature is  $T_h^* = T_h e^{2r_h}$ , while the effective lowest temperature is  $T_c^* = T_c$ .

### 5.4 How efficiency is measured

From the displacement of the oscillator, the value of the two rotating coordinates, their effective temperature, and entropy can be calculated. So, one can generate a “temperature-entropy diagram” of the cycle, and find the corresponding efficiency. One can also find

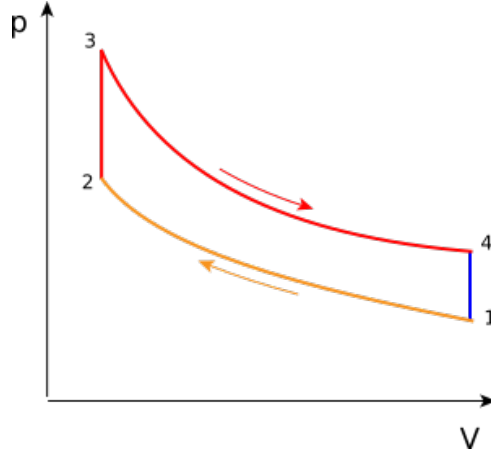


**Figure 5:** pressure-volume diagram of Otto Cycle. Image source: Wikipedia [19]

generate a “pressure-volume diagram” (where pressure and volume are defined in the last subsection), and find the efficiency from the ratio of work done (the area enclosed by the loop) and the heat supplied to the system when  $T = T_h$ . When the system is coupled to the hot bath (i.e. the prefactor  $a_0$  in the stochastic force (14) is such that  $T = T_h$ ), it undergoes an isochoric process, i.e. its volume (here inverse frequency) does not change. Then the work done is zero, and from first law of thermodynamics, the effective heat given to the system is equal to the increase in internal energy (which can be calculated using the formula of internal energy given in the last subsection).

It is experimentally found that the efficiency of the engine is more than the standard Carnot limit  $1 - \frac{T_c}{T_h}$  (although it is less than  $1 - \frac{T_c^*}{T_h^*}$ ).

## 6 Explanation of different effective temperatures and the reason for surpassing the second law

In 2.3.2 we saw that the effective temperature of the system is proportional to the square of the magnitude of the stochastic force. The force  $\xi(t) = a_0[e^{\tilde{r}}\xi_1(t)\cos(\omega t) + e^{-\tilde{r}}\xi_2(t)\sin(\omega t)]$  can be viewed as a combination of two forces with magnitudes  $a_1 = a_0e^{\tilde{r}}$  and  $a_2 = a_0e^{-\tilde{r}}$ . This is as if, the system is simultaneously coupled to two heat baths of temperatures  $Te^{2\tilde{r}}$  and  $Te^{-2\tilde{r}}$ . This gives rise to the different temperatures in the two rotating coordinates. Note that the temperatures in (40) are just linear combinations of the temperatures of

these two heat baths.

As mentioned in [2], we can only say that Carnot efficiency has been surpassed if squeezing can be obtained as a free resource. If we have two engines, one of which creates the squeezed force, and the other utilizes it, then the efficiency of the whole system will not be greater than the Carnot limit.

There is a notion of generalized Carnot limit given by  $\eta = 1 - \frac{T_c^*}{T_h^*}$  (where  $T^*$  denotes the effective temperature). It is seen that the experimental efficiency is still less than this limit, although it is more than the standard Carnot limit  $1 - \frac{T_c}{T_h}$ .

When we calculate the change in entropy, we need to take into account the effective temperatures  $T_h^*$  and  $T_c^*$  of the heat baths, and that is why, the second law of thermodynamics would not be violated. When we use this special stochastic force, the system is really coupled to two heat baths of different temperatures, and we should not compare its efficiency to the “formula” of standard Carnot efficiency, with some intermediate temperature  $T_h$  and  $T_c$ , where the squeezing parameter  $r$  is put to zero.

## 7 Conclusion

The efficiency of the heat engine was calculated from the Temperature-Entropy diagram obtained from the rotating coordinates, the heat engine was not coupled to anything that extracts actual work. Also, the effective temperatures are different in the rotating coordinates, while they are equal in the lab coordinates. It is to be investigated how work can be experimentally extracted from the rotating coordinates. Although the claim of surpassing Carnot efficiency depends on how the temperatures are interpreted, these microscopic engines can provide much higher efficiency than traditional macroscopic engines, and may become very useful in the near future.

## References

- [1] Resnick R., Halliday D., and Walker J. *Principles of Physics*, pages 525–528. Wiley, 10th edition, 2014.

- [2] Jan Klaers, Stefan Faelt, Atac Imamoglu, and Emre Togan. Squeezed thermal reservoirs as a resource for a nanomechanical engine beyond the carnot limit. *Phys. Rev. X*, 7:031044, Sep 2017.
- [3] James Millen and André Xuereb. The rise of the quantum machines. *Physics World*, 29(1):23–26, jan 2016.
- [4] O. Abah, J. Roßnagel, G. Jacob, S. Deffner, F. Schmidt-Kaler, K. Singer, and E. Lutz. Single-ion heat engine at maximum power. *Phys. Rev. Lett.*, 109:203006, Nov 2012.
- [5] Sudeesh Krishnamurthy, Subho Ghosh, Dipankar Chatterji, Rajesh Ganapathy, and A. K. Sood. A micrometre-sized heat engine operating between bacterial reservoirs. *Nature Physics*, 12(12):1134–1138, 2016.
- [6] A. del Campo, J. Goold, and M. Paternostro. More bang for your buck: Superadiabatic quantum engines. *Scientific Reports*, 4(1):6208, 2014.
- [7] J. Roßnagel, O. Abah, F. Schmidt-Kaler, K. Singer, and E. Lutz. Nanoscale heat engine beyond the carnot limit. *Phys. Rev. Lett.*, 112:030602, Jan 2014.
- [8] Cohen-Tannoudji C., Diu B., and Laloe F. *Quantum Mechanics*, volume One, chapter V. WILEY-VCH, 1977.
- [9] Wikipedia article for coherent states. [https://en.wikipedia.org/wiki/Coherent\\_states](https://en.wikipedia.org/wiki/Coherent_states).
- [10] M C Teich and B E A Saleh. Squeezed state of light. *Quantum Optics: Journal of the European Optical Society Part B*, 1(2):153–191, dec 1989.
- [11] metamorphy (<https://math.stackexchange.com/users/543769/metamorphy>). How to solve the recurrence relation  $d_n = a\sqrt{n+1}d_{n+1} + b\sqrt{n}d_{n-1}$  (when  $n \in \mathbb{Z}^+$ ), and  $d_0 := ad_1$ . Mathematics Stack Exchange. URL:<https://math.stackexchange.com/q/3344192> (version: 2019-09-04).
- [12] Arfken G. B., Weber H. J., and Harris F. E. *Mathematical Methods for Physicists*, chapter 18.1. Academic Press, 7th edition, 2013.
- [13] Wikipedia article for white noise. [https://en.wikipedia.org/wiki/White\\_noise](https://en.wikipedia.org/wiki/White_noise).

- [14] Peter Reimann. Brownian motors: noisy transport far from equilibrium. *Physics Reports*, 361(2):57 – 265, 2002.
- [15] S. Chandrasekhar. Stochastic problems in physics and astronomy. *Rev. Mod. Phys.*, 15:1–89, Jan 1943.
- [16] <https://github.com/apandada1/physics-simulations/tree/master/Brownian%20Harmonic%20oscillator>.
- [17] Wikipedia article for Runge-Kutta methods. [https://en.wikipedia.org/wiki/Runge%E2%80%93Kutta\\_methods](https://en.wikipedia.org/wiki/Runge%E2%80%93Kutta_methods).
- [18] Supplemental material of [2]. [https://journals.aps.org/prx/supplemental/10.1103/PhysRevX.7.031044/heatengine-PRX-supplemental\\_V3.pdf](https://journals.aps.org/prx/supplemental/10.1103/PhysRevX.7.031044/heatengine-PRX-supplemental_V3.pdf).
- [19] [https://commons.wikimedia.org/wiki/File:P-V\\_Otto\\_cycle.svg](https://commons.wikimedia.org/wiki/File:P-V_Otto_cycle.svg).